Rare Metal Materials and Engineering
Volume 49, Issue 8, August 2020
Available online at www.rmme.ac.cn

Science Press

Cite this article as: Rare Metal Materials and Engineering, 2020, 49(8): 2630-2635.

ARTICLE

Preparation and Structure Characteristics of Porous Monel Alloy

Guo Chaoqun, Wang Tianyao, Yuan Tianxiang, Ma Delin, Zhou Yun, Zuo Xiaoqing

Kunming University of Science and Technology, Kunming 650093, China

Abstract: In order to prepare Monel alloy porous filtration material, the porous Monel samples with different porosity were fabricated by a sintering-dissolution process using Monel powder as raw material and K_2CO_3 as a space holder. The influence of space holder, compacting pressure and sintering temperature on the porosity, cell size and permeability of samples was investigated. The results show that the porosity of samples is in range of 31%~46%, when the volume fraction of the space holder is between 20 vol% and 40 vol%. While compacting pressure in the range of 200~400 MPa, the porosity, cell size and permeability of samples decrease with compacting pressure increasing; while sintering temperature in the range of 850~1000 °C, the cell size and permeability increase first, then slowly decrease with the sintering temperature increasing, and the peak values are at 950 °C. While the volume fraction of space holder is 30%, compacting pressure is 200 MPa, sintering temperature is 950 °C, the porosity, maximum cell size and permeability of the porous Monel sample are 37%, 21.5 μm, 76.77 $m^3/(h \cdot kPa \cdot m^2)$, respectively.

Key words: Monel alloy; porous materials; K_2CO_3; porosity; filtration material

The porous metal material made up of metal matrix and internal pores is an advanced composite material having structural and functional characteristics. The porous metal materials have many advantages, such as light weight, high specific strength, large specific surface area, good sound and energy adsorption, high temperature resistance[1-5]. It can be used as light structure, filter, heat dissipating, damping and energy absorbing material for metallurgy, chemical industry, new energy, environmental protection, aerospace, electronic devices and other fields[6-8]. Filtration and separation is one of the widest fields of application for metal porous materials. The characteristics of the filter material and the distribution of the internal pore structure directly affect the filtration performance and application. At present, the filter materials widely used in industry are mainly ceramic porous filter materials and metal porous filter materials. Metal porous filter materials are mainly copper alloys, titanium alloys, stainless steels and nickel based alloys. Copper based filtration materials are basically harmless to the human body and can be used as medical filtering materials and water purification materials.

Stainless steel and nickel based alloy filter materials are excellent in high temperature and corrosion resistance. It is suitable for environmental protection, metallurgy, chemical industry, petroleum and new energy field, such as DPF system for purifying diesel exhaust, filtering blast furnace gas for an iron and steel plant, filtering tiny radioactive contaminants in the reactor purification liquid, purifying the hydraulic oil in the aircraft[9-11]. In past years, stainless steel porous materials have been being developed rapidly. Kato et al[12] fabricated porous 316L stainless steel by an original slurry foaming method, and its pore size is in the range of 50~500 μm and porosity is between 15%~95%. Ma et al[13] prepared stainless steel hollow fiber. Its porosity is between 43% and 51%, the maximum pore size ranges from 26.7 μm to 39.2 μm, and pure water flux is 3.16~26.1 (105 $L \cdot m^{-2} \cdot h^{-1} \cdot Pa^{-1}$). Ao et al[14] prepared 316L stainless steel fiber porous felts by webbing, rolling, sintering, with porosity between 60% and 90%, and pore diameter in the range of 8~12 μm. The nickel based

Received date: August 10, 2019
Foundation item: National Natural Science Foundation of China (51264024, 51861020); Innovation and Entrepreneurship Training Project for College Students (201710674207)
Corresponding author: Zhou Yun, Ph. D., Professor, Faculty of Materials Science and Engineering, Kunming University of Science and Technology, Kunming 650093, P. R. China, E-mail: zyuncrystal@qq.com; yunz@kmust.edu.cn

alloys are superior to stainless steels in performance under extremely high temperature and oxidation environment[15-17]. Recently, the porous nickel based alloys are also being developed. Yu et al[18] prepared a porous nickel-copper alloy with controlled micro-sized pore structure through the Kirkendall effect. The open porosity of the fabricated porous Ni-Cu material is between 23.5% and 37.8%, and the average pore diameter ranges from 2.6 μm to 11.8 μm. Walther et al[19] prepared nickel-based open-cell foams. The pore size is between 250 μm and 2 mm, and the maximum porosity is about 95%. Ryi et al[20] prepared nickel filters by compressing micron-size nickel powder. The porosity is between 18% and 53%, and the pore diameter is in the range of 1~10 μm.

There are some techniques for manufacturing the porous metal filters, including powder sintering and combustion technique[20,21], fiber sintering methods[22], metallorganic salts decomposition[23], the de-alloying method[24] and so on. However, these methods are complex and costly, and it is difficult to control porosity and pore structure. This work attempts to use a simple method to manufacture porous Monel filter material. This method includes four steps: blending, compacting, sintering and removing space holder. The space holder selected in this work is K_2CO_3 particles. K_2CO_3 has good chemical stability, high melting point (891 °C), non-toxic, good water solubility and low cost, which is an ideal space holder. It is practicable to control porosity and pore structure of porous filter material by changing the amount and size of space holders. The purpose of this study is to prepare a porous Monel material with predetermined porosity and pore shape. The effects of the process parameters (space holder, pressing pressure, sintering temperature) on the porosity, maximum cell size and permeability coefficient were investigated.

1 Experiment

Monel alloy powder (purity≥99.9%, particle size 40~50 μm, density 8.9 g/cm^3) was used as raw materials and K_2CO_3 (purity≥99.9%, particle size 50~70 μm, density 2.428 g/cm^3) was used as space holders.

Monel alloy powder and K_2CO_3 particle were mixed according to the volume ratio, and ethanol was added as a binder during mixing processing. The addition amount of the binder was 2 wt%~5 wt%. The mixed powder was compacted by unidirectional cold-pressing in a cylindrical die, with 32~50 mm in diameter, compacting pressure 200~400 MPa, holding time 3~5 min, and then the binder was vaporized in a drying oven at 120 °C for 2~4 h. The dried compacts were sintered in argon atmosphere at 850~1000 °C for 1~3 h. The sintered specimens were subsequently placed into running water to dissolve residual K_2CO_3. The microstructure and composition were analyzed using SEM (Quanta200, Holland) and XRD (XL30ESEM-TMP, Holland).

The porosity of the samples were measured by Archimedes drainage[25,26]. Firstly the mass of porous samples (m_0) was weighed, and then they were soaked in the oil for 24 h, until the pores of the samples were completely filled by the oil. Secondly the samples were taken out, the oil drops on the surface were gently wiped off, and the mass of the samples filled with oil (m_1) was weighed. Finally the samples were hanged with fine wire and put into pure water, and then the mass of the samples (m_2) was weighed. The porosity of open cells is calculated by Eq. (1)[26].

$$\theta_k = \frac{\rho_1(m_1 - m_0)}{\rho_2(m_1 - m_2)} \times 100\% \quad (1)$$

where, θ_k-porosity of open cells; m_0-the mass of the sample in the air; m_1-the mass of sample filled by the oil; m_2-the mass of oil immersed samples hanged in water; ρ_1-water density; ρ_2-oil density.

The total porosity is calculated by Eq. (2)[26].

$$\theta = \left[1 - \frac{\rho_1 m_0}{\rho_s(m_1 - m_2)}\right] \times 100\% \quad (2)$$

where, θ-total porosity of porous materials; ρ_s-the density of metal solid material.

The percentage of opening (η) is the percentage of the porosity of open cells to the total porosity, calculated by Eq. (3)[26].

$$\eta = \frac{\theta_k}{\theta} \times 100\% \quad (3)$$

The maximum cell diameter and permeability coefficient were measured by FBP3I instrument provided by Northwest Institute for Nonferrous Metal Research. The maximum cell diameter is calculated by Eq. (4)[27].

$$d = \frac{4r\cos\theta}{\Delta p} \quad (4)$$

where, d-the maximum cell diameter corresponding to the minimum bubble pressure (Δp); r-surface tension of experimental liquid, N/m; θ-wetting angle. The permeability coefficient is calculated by Eq. (5)[27].

$$K_g = \frac{Q}{A\Delta p} \quad (5)$$

where, K_g-permeability coefficient, m^3/(h·kPa·m^2); Q-gas flow, m^3/h; A-the area of gas passing, m^2; Δp-pressure difference acting on both sides of porous sample, kPa.

2 Results and Discussion

2.1 Microstructure

The obtained samples are shown in Fig.1, whose porosity is 31%~46%, diameter 30~32 mm, and thickness 1.5~3.5 mm. It can be seen that the samples are flat and no cracks appear.

Fig.2 shows the SEM micrographs of porous samples. It can be observed that pores are evenly distributed in the matrix from Fig.2a and 2b. Fig.2c shows that metal particles are bonding together to form matrix at sintering temperature 1000 °C for 2 h. The large-sized pores are formed by removing space holders, and some tiny pores on the matrix by sintering

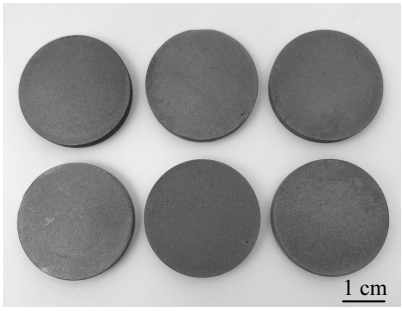

Fig.1 Porous Monel samples

shrinkage of metal particles. It indicates that the required filter materials can be fabricated by the method.

2.2 XRD

Fig.3 is XRD pattern of porous samples. It is known that the phase is only one Ni(Cu) solid solution. The Ni-Cu phase diagram shows that Ni and Cu are infinitely intersoluble, and Cu atoms are fully dissolved in the Ni matrix to form a solid solution. There is only Ni(Cu) solid solution and no other phases are found in Fig.3. It is believed that the space holder has been removed from matrix, and there are not any chemical reactions between the space holder and matrix. It is found that that K_2CO_3 is an ideal space holder.

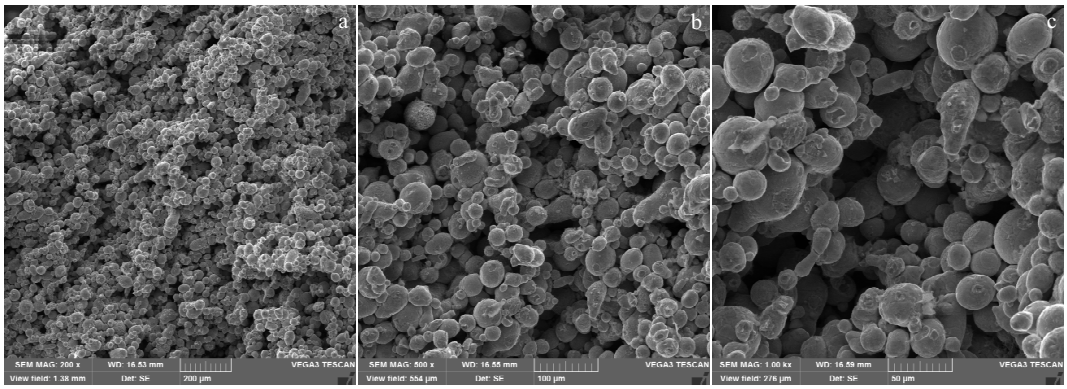

Fig.2 SEM micrographs of porous samples sintered at 1000 °C for 2 h

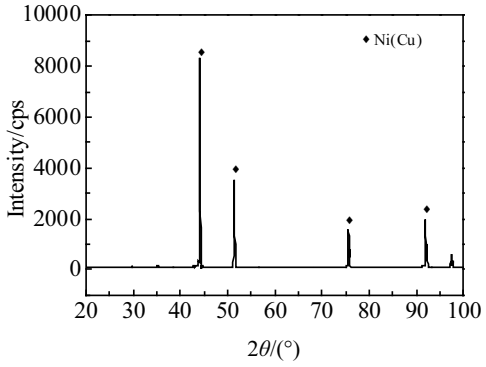

Fig.3 XRD pattern of porous Monel sample

2.3 Influence factors of porosity

2.3.1 Volume fraction of space holder

For porous filtration materials, the fluid flow is proportional to the porosity. As porosity increases, the strength of the porous material decreases. In order to balance the permeability and strength of the filter material, generally, the porosity of the porous materials is not more than 50%. When studying the effect of volume fraction of space holder on porosity, the compacting pressure and sintering temperature were held constant, which were 200 MPa and 900 °C, respectively. The volume fraction of the space holder K_2CO_3 was determined to be 20%, 30%, 35% and 40%.

Fig.4 shows the relationship between the porosity and volume fraction of space holder of porous material. When the amount of space holder is in the range of 20~40 vol%, the porosity is 31%~46%. The porosity increases with the increase of volume fraction of space holder. The porosity varies almost linearly with the volume fraction of space holders.

Since the pore structure of samples is mainly formed by removing space holders, it is possible to control the porosity

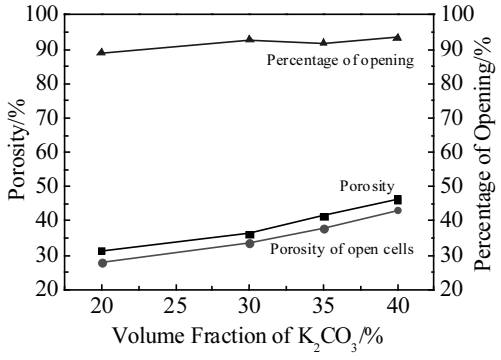

Fig.4 Relationship between porosity, percentage of opening and K_2CO_3 volume fraction

of samples by controlling the amount of space holders, and to prepare porous materials with corresponding porosity for requirements.

The percentage of opening (η) is the percentage of the porosity of open cells in the total porosity. Fig.4 shows that the percentage of opening (η) is more than 89% when the volume fraction of space holder K_2CO_3 is in the range of 20%~40%. It indicates that the porous materials prepared by this method are basically open cell structures.

2.3.2 Compacting pressure

In order to study the effect of compacting pressure on porosity, the volume fraction of the space holder and sintering temperature were held constant, which were 30% and 900 °C, respectively. The compacting pressure was determined to be 200, 300 and 400 MPa, with the holding time 3 min. The porosity varying with compacting pressures is shown in Fig.5. It shows that the porosity of porous samples decreases with the compacting pressure increasing. The main reason is that the total volume of the green compact shrinks and the density increases with the compacting pressure increasing, leading to the decrease of sample porosity. When the compacting pressure increases from 200 MPa to 300 MPa, the porosity decreases rapidly; the compacting pressure increases from 300 MPa to 400 MPa, and the porosity declines slowly.

2.3.3 Sintering temperature

Generally, the sintering temperature is in the range of 0.6~0.8 times of the melting point of solid material. In order to investigate the influence of sintering temperature on porosity, the compaction pressure and the space holder volume fraction were held constant, which were 200 MPa and 30%, respectively. The samples were sintered at 850, 900, 950, and 1000 °C. Fig.6 shows the effect of sintering temperature on porosity of porous samples. When the sintering temperature increases from 850 °C to 900 °C, the porosity decreases rapidly; when temperature increases from 900 °C to 950 °C, the porosity decreases slowly; when temperature increases from 950 °C to 1000 °C, the porosity decreases again rapidly. It is obvious that the volume shrinkage of samples is significant at the initial temperature sintering (850 °C to 900 °C) and high temperature (above 950 °C) sintering stage.

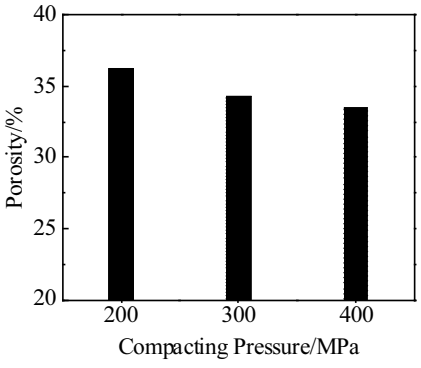

Fig.5 Relationship between porosity and compacting pressure

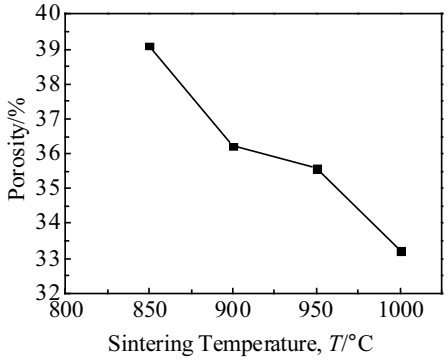

Fig.6 Relationship between porosity and sintering temperature

2.4 Influence factors of filtering characteristic parameters

2.4.1 Volume fraction of space holder

Filtering precision is a key parameter of metal porous material in practical application. One of its definitions is the maximum particle size allowed to pass or the minimum particle size intercepted, and usually denoted by the maximum cell size, called absolute filtering precision[28]. In this paper, a bubble method was used to determine the maximum cell size of filter materials. The larger the maximum cell size is, the larger the particle that can pass through. When the average cell size of the sample is certain, the smaller the maximum cell size is, the higher the filtering precision is. Table 1 shows the influence of the volume fraction on the filtering parameters. It can be seen that the average cell size, the maximum cell size and the air permeability increase with the increase of the volume fraction of space holder. The amount of space holder has an obvious influence on the air permeability. When the amount of the space holder is 20 vol%, the average cell size is 3.9 μm, the maximum cell size is 19.2 μm, and the permeability is 21.65 $m^3/(h\cdot kPa\cdot m^2)$. When the amount of space holder is 40 vol%, the average cell size is 6.2 μm, the maximum cell size is 24.7 μm, and the permeability is 131.95 $m^3/(h\cdot kPa\cdot m^2)$. As the amount of space holder increases from 20 vol% to 40 vol%, the air permeability is increased by about 6 times.

2.4.2 Compacting pressure

Table 2 shows the influence of compacting pressure on the filtering parameters of porous samples. The volume fraction of space holder and sintering temperature were constant, which were 30 vol% and 900 °C, respectively. While the pressing pressure is 200 MPa, the average cell size is 5 μm, the maximum

Table 1 Effect of K_2CO_3 volume fraction on filtering characteristic parameters

Volume fraction of space holder/%	20	30	40
Average cell size/μm	3.9	5	6.2
Maximum cell size/μm	19.2	21.2	24.7
Air permeability/$m^3\cdot(h\cdot kPa\cdot m^2)^{-1}$	21.65	56.66	131.95

Table 2 Effect of compacting pressure on filtering characteristic parameters

Compacting pressure/MPa	200	300	400
Average cell size/μm	5	3.5	3.1
Maximum cell size/μm	21.2	17.1	16.5
Air permeability/$m^3\cdot(h\cdot kPa\cdot m^2)^{-1}$	56.66	33.51	31.52

cell size is 21.2 μm, and the permeability 56.66 $m^3/(h\cdot kPa\cdot m^2)$; when the pressure increases to 400 MPa, the average cell size is 3.1 μm, the maximum cell size is 16.5 μm, and the permeability is 31.52 $m^3/(h\cdot kPa\cdot m^2)$. It is found that the average cell size, the maximum cell size and the permeability decrease with the increase of pressure. While the compacting pressure is lower, the density of green compact is low, a large number of pores are retained in the compact and is not easy to close during sintering, so the maximum cell size and the permeability are higher. With the increase of compacting pressure, the density of the green compact increases and metal particles are bound tightly, so the cell sizes and the air permeability decrease after sintering.

2.4.3 Sintering temperature

Table 3 shows the influence of sintering temperature on the filtering parameters of porous samples. The compacting pressure and the volume fraction of the space holder were constant, which were 200 MPa and 30 vol%, respectively. It can be seen that the average cell size of porous increases from 4.4 μm to 5.6 μm, the maximum cell size from 20.6 μm to 21.5 μm, and the air permeability from 43.35 $m^3/(h\cdot kPa\cdot m^2)$ to 76.77 $m^3/(h\cdot kPa\cdot m^2)$ while the sintering temperature rises from 850 °C to 950 °C. However, when the sintering temperature continuously goes up to 1000 °C, the average cell size, maximum cell size, and air permeability start to decrease. This phenomenon can be explained as: while sintering temperature is 850~950 °C, with the temperature increasing, atoms diffusion rate is accelerated, and the distance of atoms migration increases, atoms on a convex surface easily diffuse to surface of neighboring large particles, and thus the sintering neck is formed, the inner surface of pores becomes smooth to form columnar channels which increases the cell diameter and permeability. As temperature rises further, the distance of atomic motion increases and the binding area between metal particles enlarges further, leading to many tiny pores closed, the cell size and permeability of samples decrease.

Table 3 Effect of sintering temperature on filtering characteristic parameters

Sintering temperature/°C	850	900	950	1000
Average cell size/μm	4.4	5	5.6	4.7
Maximum cell size/μm	20.6	21.2	21.5	20.9
Air permeability/$m^3\cdot(h\cdot kPa\cdot m^2)^{-1}$	43.35	56.66	76.77	44.02

3 Conclusions

1) The porous Monel samples were successfully fabricated, with the porosity 31%~46%, the percentage of open cell more than 89%, diameter 30~32 mm and thickness 1.5~3.5 mm.

2) The main factors affecting porosity are the volume fraction of space holder, compacting pressure, and sintering temperature. The porosity increases with the increase of space holder volume fraction, and decreases with the increase of compacting pressure and sintering temperature.

3) The maximum cell size and permeability of porous Monel increase with increasing volume fraction of space holder, and decrease with compacting pressure increasing. While sintering temperature is between 850~1000 °C, the maximum cell size and permeability of porous Monel increases first, then slowly decreases, and the peak value is at 950 °C.

4) While the volume fraction of space holder is 30%, compacting pressure is 200 MPa, sintering temperature is 950 °C, the porosity, maximum cell size and the permeability of the porous Monel sample reach 37%, 21.5 μm and 76.77 $m^3/(h\cdot kPa\cdot m^2)$, respectively.

References

1 Nakajima H. *Progress in Materials Science*[J], 2017, 52(7): 1091
2 Banhart J. *Progress in Materials Science*[J], 2001, 46(6): 559
3 Qin J H, Chen Q, Yang C Y *et al*. *Journal of Alloys and Compounds*[J], 2016, 654: 39
4 Choi S H, Kim S Y, Yun J Y *et al*. *Metals and Materials International*[J], 2011, 17(2): 301
5 Li J X, Zhao S D, Ishihara K. *Journal of Sound and Vibration*[J], 2013, 332(11): 2721
6 Jabur A S. *Powder Technology*[J], 2013, 237: 477
7 Abdullah Z, Ismail A, Ahmad S. *Journal of Physics: Conference Series*[J], 2017, 914: 012 013
8 Oun H, Kennedy A R. *Journal of Porous Materials*[J], 2014, 21(6): 1133
9 García-Moreno F. *Materials*[J], 2016, 9(2): 85
10 Kavanagh P R, Brown D E. *Journal of Chemical Technology and Biotechnology*[J], 1987, 38(3): 187
11 Song T, Xiong W, Han J. *Atomic Energy Science and Technology*[J], 2010, 44(11): 1397
12 Kato K, Yamamoto A, Ochiai S *et al*. *Materials Science and Engineering C*[J], 2013, 33(5): 2736
13 Ma X H, Bai Y, Cao Y *et al*. *Korean Journal of Chemical Engineering*[J], 2014, 31: 1438
14 Ao Q B, Tang H P, Wang J Z *et al*. *Rare Metal Materials and Engineering*[J], 2014, 43(10): 2344
15 Heikkinen M S A, Harley N H. *Journal of Aerosol Science*[J], 2000, 31(6): 721
16 Pang Q, Wu G H, Xiu Z Y *et al*. *Materials Characterization*[J], 2012, 70: 125
17 Gourgues A F, Andrieu E. *Materials Science and Engineering*

A[J], 2003, 351(1-2): 39
18 Yu L, Jiang Y, He Y *et al*. *Materials Chemistry and Physics*[J], 2015, 163: 355
19 Walther G, Klöden B, Büttner T *et al*. *Advanced Engineering Materials*[J], 2008, 10(9): 803
20 Ryi S K, Park J S, Park S J *et al*. *Journal of Membrane Science*[J], 2007, 299(1-2): 174
21 Nersisyan H H, Won H I, Won C W *et al*. *Materials Chemistry and Physics*[J], 2013, 141(1): 283
22 Chen C, Yang J F, Chu C Y *et al*. *Materials Chemistry and Physics*[J], 2011, 128: 24
23 Bonino F, Chavan S, Vitillo J G *et al*. *Chemistry of Materials*[J], 2008, 20(10): 4957
24 Erlebacher J, Aziz M J, Karma A *et al*. *Nature*[J], 2001, 410: 450
25 Mulder M. *Basic Principles of Membrane Technology*[M]. Netherlands: Springer, 1996
26 Xi Z P, Tang H P. *Sintered Metal Powder Porous Media*[M]. Beijing: Metallurgical Industry Press, 2009 (in Chinese)
27 Venkataraman K, Choate W T, Torre E R *et al*. *Journal of Membrane Science*[J], 1988, 39(3): 259
28 Sun T, Xi Z P, Tang H P *et al*. *Rare Metal Materials and Engineering*[J], 2008, 37(S4): 509 (in Chinese)

多孔蒙乃尔合金的制备及其结构特性

郭超群，汪天尧，袁天祥，马德林，周　芸，左孝青
(昆明理工大学，云南 昆明 650093)

摘　要：以蒙乃尔粉为原料，以 K_2CO_3 为造孔剂，采用烧结-溶解法制备了不同孔隙率的蒙乃尔合金多孔试样。研究了造孔剂体积分数、压坯压力和烧结温度对试样孔隙率、孔径和透气度的影响。结果表明，当造孔剂的体积分数在 20%~40%之间时，制备的样品孔隙率为 31%~46%。当压坯压力在 200~400 MPa 范围时，随压力的增大试样的孔隙率、孔径和透气度均减小；当烧结温度在 850~1000 ℃范围时，随烧结温度升高，孔径和透气度先增大后缓慢降低，在 950 ℃达到峰值。当造孔剂体积分数为 30%，压制压力为 200 MPa，烧结温度 950 ℃时，所制备的蒙乃尔多孔材料孔隙率为 37%，最大孔径为 21.5 μm，透气度为 76.77 $m^3/(h·kPa·m^2)$。

关键词：蒙乃尔合金；多孔材料；碳酸钾；孔隙率；过滤材料

作者简介：郭超群，女，1994 年生，硕士生，昆明理工大学材料科学与工程学院，云南 昆明 650093，E-mail: 793103029@qq.com